Molecular Microbiology (2005) **58**(1), 28–45

doi:10.1111/j.1365-2958.2005.04742.x
First published online 17 August 2005

Analysis of *Xenorhabdus nematophila* metabolic mutants yields insight into stages of *Steinernema carpocapsae* nematode intestinal colonization

Eric C. Martens, Frances M. Russell and Heidi Goodrich-Blair*
Department of Bacteriology, University of Wisconsin, Madison, WI 53706, USA.

Summary

Xenorhabdus nematophila **colonizes the intestinal tract of infective-juvenile (IJ) stage** ***Steinernema carpocapsae*** **nematodes. During colonization,** ***X. nematophila*** **multiplies within the lumen of a discrete region of the IJ intestine termed the vesicle. To begin to understand bacterial nutritional requirements during multiplication in the IJ vesicle, we analysed the colonization behaviour of several** ***X. nematophila*** **metabolic mutants, including amino acid and vitamin auxotrophs.** ***X. nematophila*** **mutants defective for para-aminobenzoate, pyridoxine or L-threonine biosynthesis exhibit substantially decreased colonization of IJs (0.1–50% of wild-type colonization). Analysis of** ***gfp*****-labelled variants revealed that those mutant cells that can colonize the IJ vesicle differ noticeably from wild-type** ***X. nematophila*****. One aberrant colonization phenotype exhibited by the metabolic mutants tested, but not wild-type** ***X. nematophila*****, is a spherical shape indicative of apparently non-viable** ***X. nematophila*** **cells within the vesicle. Because these spherical cells appear to have initiated colonization but failed to proliferate, we term this type of colonization 'abortive'. In a portion of IJs grown on para-aminobenzoate auxotrophs,** ***X. nematophila*** **does not exhibit abortive colonization but rather reduced growth and filamentous cell morphology. Several mutants with defects in other amino acid, vitamin and nutrient metabolism pathways colonize IJs to wild-type levels suggesting that the IJ vesicle is replete with respect to a number of nutrients.**

Accepted 23 May, 2005. *For correspondence. E-mail hgblair@bact.wisc.edu; Tel. (+1) 608 265 4537; Fax (+1) 608 262 9865.

Introduction

The entomopathogenic nematode, *Steinernema carpocapsae*, associates mutualistically with the Gram-negative enterobacterium *Xenorhabdus nematophila*, and together these two species proliferate by parasitizing and reproducing inside a number of insect species (Poinar, 1966; Poinar and Thomas, 1966; Forst and Clarke, 2002). A non-feeding, environmentally resistant form of *S. carpocapsae*, the infective juvenile (IJ), carries a microcolony of *X. nematophila* in a discrete intestinal location (vesicle) and serves as a vector for these bacteria between hosts. Infection is initiated when IJs invade an insect host and release their intestinal *X. nematophila* into the insect haemolymph, an event resulting in insect death. *S. carpocapsae* develops through multiple growth stages that feed on the *X. nematophila* cells that have proliferated to high cell density inside the cadaver. When nematode populations become crowded and/or starved for nutrients, IJs develop in the spent insect cadaver and during this process reassociate with their mutualistic *X. nematophila* (Popiel *et al*., 1989; Martens *et al*., 2003a). IJs then migrate into the environment, carrying *X. nematophila* in their intestines, to infect new insect hosts.

We are investigating the *S. carpocapsae–X. nematophila* mutualism as a model of the process through which an aposymbiotic host (feeding nematode) acquires its symbiont as it develops into a colonized state (the IJ) (Vivas and Goodrich-Blair, 2001). Attractive features of this model system are that it consists of only two species (nematode and bacteria) and that it is species-specific such that other bacteria, including related *Xenorhabdus* spp., are excluded from colonizing the *S. carpocapsae* IJ intestinal vesicle (Poinar and Thomas, 1966; Grewal *et al*., 1997; Sicard *et al*., 2004a). Thus, these two organisms provide a simple, specific model of host–microbe recognition during the colonization process.

We previously described early stages in the process through which *X. nematophila* colonizes the IJ intestine (Martens *et al*., 2003a). These stages include an initiation event, whereby one (or a few) *X. nematophila* cell is retained in the intestinal vesicle of a developing IJ, and an outgrowth phase, where the initial colonizer(s) prolifer-

ates in the IJ intestine to produce a full population of bacteria (≥40 viable *X. nematophila* cells per IJ). For *X. nematophila* to proliferate in the nematode intestine, it must access available nutrients required for growth. The presence and chemical nature of a putative nutrient source(s) within the IJ vesicle remains unexplored. However, a previous morphological investigation suggests that in some *Steinernema* spp. the vesicular lumen contains an amorphous matrix, which is observed in both the presence and absence of colonizing *Xenorhabdus* spp. (Bird and Akhurst, 1983). Bacteria that occupy the IJ vesicle are found embedded within this matrix (Bird and Akhurst, 1983) and likely use either it or other host-secreted compounds as a nutrient source(s) during *in vivo* growth.

In systems where microbes proliferate within host species, it is useful to understand the basis of how colonizing microbes harvest nutrients from their hosts. Such an understanding may shed light on why particular microbial species occupy a host niche to the exclusion of others (specificity), and how colonization is limited to certain host niches (tropism). In other models of mutualistic bacterial–host associations, insights into both host–bacteria nutrient exchange and bacterial nutritional requirements during colonization have been gained by analysing the ability of auxotrophic bacterial mutants to colonize their host (Graf and Ruby, 1998; 2000; Ferraioli *et al*., 2002). In such experiments, two possible outcomes are anticipated. The first is that a particular auxotroph colonizes its host similarly to its wild-type parent, yielding the conclusion that the nutrients required by that auxotroph are supplied in adequate amounts within its host. The second possible outcome is that a particular auxotroph fails to colonize its host as well as its wild-type parent, suggesting that the nutrient(s) required by that auxotroph is either unavailable or limiting within the host environment. Thus, the simple logic of testing the colonization abilities of defined auxotrophs provides a mechanism for probing the nutrient composition of the host environment. Such a molecular genetic approach to define the nutritional composition of the host environment is particularly attractive in the *X. nematophila–S. carpocapsae* mutualism because the small size (~0.5 mm overall length) of the nematode renders it recalcitrant to biochemical studies of intestinal contents and tissues.

In a previous study, we identified two colonization-deficient *X. nematophila* mutants harbouring Tn*5* insertions in *serC* or *aroA*, putatively required for L-serine and aromatic amino acid biosynthesis respectively (Heungens *et al*., 2002). Based on functions of homologous genes in *Escherichia coli*, *serC* is predicted to encode phosphoserine transaminase (hereinafter referred to as SerC), an enzyme involved in both L-serine and pyridoxine biosynthesis (Hill and Spenser, 1996; Stauffer, 1996). *aroA* is predicted to encode 5-enoylpyruvoylshikimate-3-phosphate synthase (hereinafter referred to as AroA), an enzyme catalysing the sixth step of the common (shikimate) branch of aromatic amino acid biosynthesis (Pittard, 1996).

We wished to investigate these two mutants (*serC* and *aroA*) as prototypic metabolic mutants defective for IJ colonization. However, a challenge in interpreting the defects associated with lack of SerC and AroA is that, in *E. coli*, these enzymes function not only in L-serine and aromatic amino acid biosynthesis, but also in production of other metabolites, including catecholate siderophores (both AroA and SerC) (Earhart, 1996), the respiratory quinones ubiquinone and menaquinone (AroA) (Meganathan, 1996), and the vitamins/vitamin precursors para-aminobenzoate and tetrahydrofolate (AroA) (Green *et al*., 1996) and pyridoxine (SerC) (Hill and Spenser, 1996). Thus, the IJ colonization defect associated with *X. nematophila serC* and *aroA* mutants could be associated with a deficiency in any of these compounds.

To clarify the roles of *X. nematophila* SerC and AroA in IJ colonization, as well as evaluate the colonization abilities of other *X. nematophila* amino acid auxotrophs, we employed a bilateral experimental approach. The first part of this approach was to characterize the colonization defects associated with loss of SerC and AroA and to isolate new mutants in the individual biosynthetic pathways that operate downstream of the reactions catalysed by these two enzymes. This allowed us to individually test the roles of metabolites derived via these pathways and clarify which are required for IJ colonization. The second part of this approach was to isolate additional amino acid and vitamin auxotrophs in pathways unrelated to SerC and AroA, allowing us to test the importance of other *X. nematophila* biosynthetic pathways in IJ colonization.

Results

serC *and* aroA *are independently required for nematode colonization*

Xenorhabdus nematophila strains HGB316 and HGB317 (Table 1) contain Tn*5* insertions in *serC* and *aroA* respectively. Testing of HGB316 and HGB317 on defined media (Orchard and Goodrich-Blair, 2004) demonstrated that these strains are auxotrophs for either L-serine or the aromatic amino acids L-tryptophan, L-phenylalanine and L-tyrosine respectively. The *serC* and *aroA* open reading frames (ORFs) are adjacent and tandem in the chromosome (Heungens *et al*., 2002) (Fig. 1A), suggesting that they may be cotranscribed in *X. nematophila* as they are in *E. coli* and *Salmonella enterica* (Hoiseth and Stocker,

Table 1. Strains and plasmids used in this study.

Strain or plasmid	Relevant features	Source or reference
HGB081	Spontaneous Rif^r mutant of *X. nematophila* AN6/1; wild-type strain	S. Forst
Metabolic mutants		
HGB316	HGB081 *serC1*::Tn*5*-kan	Heungens *et al*. (2002)
HGB317	HGB081 *aroA1*::Tn*5*-kan	Heungens *et al*. (2002)
HGB647	HGB081 *aroE5*::Tn*5*-cml	This study
HGB674	HGB081 *trpE2*::Tn*5*-cml	This study
HGB683	HGB081 *panB1*::Tn*5*-kan	This study
HGB731	HGB081 *leuB1*::Tn*5*-cml	Orchard and Goodrich-Blair (2004)
HGB821	HGB081 *pabA1*::Tn*10*-kan	This study
HGB823	HGB081 *thrC1*::Tn*5*-kan	This study
HGB825	HGB081 Δ *tyrA-pheA*	This study
HGB826	HGB674 Δ *tyrA-pheA*	This study
HGB956	HGB081 *serB2*::pDel-1KS	This study
HGB958	HGB081 *hisB1*::Tn*10*-kan	This study
HGB959	HGB081 *cysJ1*::Tn*10*-kan	This study
HGB961	HGB081 *ilvC1*::Tn*5*-kan	This study
HGB962	HGB081 *ubiC1*::pDel-1KS	This study
HGB963	HGB081 *menF1*::pDel-1KS	This study
HGB964	HGB081 *kbl1*::pDel-1KS	This study
HGB965	HGB081 *tonB1*::pDel-1KS	This study
Other mutants		
HGB166	HGB081 *iscRSUA*::Tn*10*-cml::*hscBA-fdx*	Martens *et al*. (2003b)
HGB310	HGB081 *nilA1*::Tn*5*-kan	Heungens *et al*. (2002)
HGB311	HGB081 *nilB2*::Tn*5*-kan	Heungens *et al*. (2002)
HGB315	HGB081 *nilD6*::Tn*5*-kan	Heungens *et al*. (2002)
HGB323	HGB081 *rpoS1*::Tn*5*-kan	Heungens *et al*. (2002)
gfp-labelled strains		
HGB338	HGB081 (wild-type)::P_{kan}-*gfp*; labelled with pECM20	This study
HGB644	HGB317 (*aroA1*)::P_{kan}-*gfp*; labelled with pECM20	This study
HGB645	HGB316 (*serC1*)::P_{kan}-*gfp*; labelled with pECM20	This study
HGB692	HGB647 (*aroE5*)::P_{kan}-*gfp*; labelled with pECM21	This study
HGB693	HGB311 (*nilB2*)::P_{kan}-*gfp*; labelled with pECM20	This study
HGB694	HGB310 (*nilA1*)::P_{kan}-*gfp*; labelled with pECM20	This study
HGB695	HGB166 (*iscRSUA*::Tn*10*-cml::*hscBA-fdx*)::P_{kan}-*gfp*; labelled with pECM21	This study
HGB698	HGB323 (*rpoS1*)::P_{kan}-*gfp*; labelled with pECM20	This study
HGB822	HGB821 (*pabA1*)::P_{kan}-*gfp*; labelled with pECM20	This study
HGB824	HGB823 (*thrC1*)::P_{kan}-*gfp*; labelled with pECM20	This study
HGB828	HGB826 (*trpE2* Δ*tyrA-pheA*)::P_{kan}-*gfp*; labelled with pECM21	This study
HGB829	HGB315 (*nilD6*)::P_{kan}-*gfp*; labelled with pECM20	This study
HGB868	HGB674 (*trpE2*)::P_{kan}-*gfp*; labelled with pECM21	This study
HGB870	HGB825 (Δ*tyrA-pheA*)::P_{kan}-*gfp*; labelled with pECM21	This study
Plasmids		
pKV124	Tn*10*-cml delivery plasmid	Visick and Skoufos (2001)
pSAG-1	Tn*10*-kan delivery plasmid	This study
pBSL203	Tn*5*-cml delivery plasmid	Alexeyev *et al*. (1995)
pBSL118	Tn*5*-kan delivery plasmid	Alexeyev *et al*. (1995)
pKR100B	*ori* R6K-based suicide vector, Cml^r	Martens *et al*. (2003a)
pHRP317	Source of Str^r cassette	Parales and Harwood (1993)
pKR100B-Str	Str^r derivative of pKR100B	This study
pRES1	Source of *kan-sacB* fragment	Andrew Camilli
pEVS107	Contains Tn*7* used for complementation	McCann *et al*. (2003)
pUX-BF13	Tn*7* transposition helper plasmid	Bao *et al*. (1991)
pDel-1KS	Derivative of pKR100B with *kan-sacB* replacing *cat*; used for insertion-duplication and deletion mutagenesis	This study
pECM20	Cml^r *gfp*-labelling construct for *X. nematophila*	Martens *et al*. (2003a)
pECM21	Kan^r *gfp*-labelling construct for *X. nematophila*	This study

1985; Duncan and Coggins, 1986). In support of this idea, reverse transcription polymerase chain reaction (RT-PCR) analysis of total bacterial RNA extracted from log-phase *X. nematophila* indicated a cotranscript containing portions of both *serC* and *aroA* (data not shown). However, HGB316 does not exhibit a requirement for aromatic amino acids on defined media, suggesting that the Tn*5* insertion in *serC* within this strain is non-polar onto *aroA*.

To clarify this issue, we performed complementation experiments with either the entire *serC-aroA* locus or the *serC* gene alone (Fig. 1A and B). The colonization defects

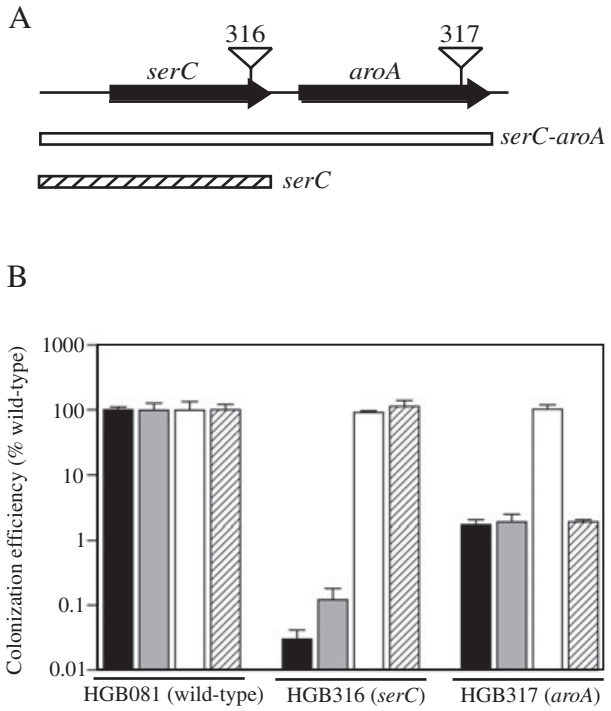

Fig. 1. *Xenorhabdus nematophila serC-aroA* locus and genetic complementation.
A. Location of Tn*5* insertions in *serC* (HGB316) and *aroA* (HGB317) are indicated by triangular symbols above each gene (represented by arrows) and labelled with the corresponding strain numbers (316 and 317). Chromosomal fragments used for mutant complementation contain either the entire *serC-aroA* locus (open bar) or *serC* only (hatched bar) and are indicated below the locus schematic. Fragment sizes and positions are approximately to scale.
B. Complementation of HGB316 and HGB317 mutant defects with *serC-aroA* locus fragments. Complementing fragments were delivered to the chromosome *in trans* to the neutral *att* Tn*7* site using transposon Tn*7* as a delivery vehicle. IJ colonization by complemented mutants is reported as colonization efficiency (*Experimental procedures*). Colonization efficiency values were determined by comparing each mutant strain with a wild-type HGB081 parent carrying an identical complementing construct where applicable. Strains contained either no Tn*7* vector (black bars), empty Tn*7* vector (grey bars), Tn*7-serC-aroA* (open bars) or Tn*7-serC* (hatched bars). Note that the actual numbers of colonizing cfu per IJ among different wild-type strains did not vary appreciably.

associated with both HGB316 and HGB317 were fully complemented by a single copy of the entire *serC-aroA* region. The mutant phenotype of HGB316 (*serC*) was also restored to wild-type levels by addition of a single copy of just *serC*, suggesting that the nematode colonization defect associated with this mutant is caused by a lack of *serC* expression. Deficient colonization by HGB317 (*aroA*) was unaffected by addition of *serC* only. Thus, although a *serC-aroA* cotranscript is identifiable in *X. nematophila*, either an endogenous (i.e. upstream of *aroA* and downstream of the *serC*::Tn*5* insertion) or exogenous (i.e. contained in Tn*5*) promoter must provide sufficient *aroA* expression in HGB316 to make it prototrophic for aromatic amino acids and colonization proficient in the presence of an uninterrupted copy of *serC*.

Metabolic defects associated with lack of serC *and* aroA

The individual requirements of SerC and AroA for normal colonization could be attributed to one or more metabolic defects associated with their respective mutations (Fig. 2). For example, wild-type *X. nematophila* could require the products of these genes for *in vivo* production of (i) *de novo* amino acids (e.g. L-serine and aromatic amino acids); (ii) a shared product arising from both the L-serine pathway and the shikimate pathway (e.g. a catecholate siderophore such as enterobactin); or (iii) synthesis of other downstream products of the AroA-catalysed reaction (cellular quinones or tetrahydrofolate) and SerC-catalysed reactions (pyridoxine or glycine).

To assist in resolving these possibilities, we performed *in silico* analysis of the incomplete *X. nematophila* ATCC 19061 genome (http://xenorhabdus.danforthcenter.org), performing searches for *X. nematophila* genes that are homologous to known biosynthetic pathways in *E. coli* and other organisms (*Experimental procedures*). We identified *X. nematophila* genes encoding putative enzymes belonging to individual pathways for biosynthesis of L-serine, L-tryptophan, L-tyrosine, L-phenylalanine, ubiquinone, menaquinone, tetrahydrofolate and pyridoxine (Fig. 2). However, probe sequences from several different bacterial species (Crosa and Walsh, 2002) failed to detect in *X. nematophila* the presence of genes encoding initial steps in the production of catecholate or salicylate siderophores. We did detect genes that likely encode biosynthetic functions for a hydroxamate siderophore (unlikely to be derived from chorismate) as well as citrate-mediated ferric-iron uptake (data not shown). We also identified a putative *tonB* gene (*Experimental procedures*), the product of which would be expected to participate in multiple, independent iron-acquisition pathways (Postle and Kadner, 2003).

Isolation of additional metabolic mutants

To further test the relevance of the shikimate pathway in IJ colonization and to begin to test the relevance of individual aromatic amino acid and vitamin auxotrophies, we screened a Tn*5*-mutagenized library of *X. nematophila* for mutants defective in aromatic amino acid biosynthesis. Of 875 mutants screened, we identified three (0.34%) that require aromatic amino acids (Table 1). One mutant, containing an insertion in *aroE,* required all three aromatic amino acids for growth on defined media. Another mutant with an insertion in *trpE* required only L-tryptophan for growth on defined media. After screening an additional 2800 Tn*5* and Tn*10* mutants we failed to isolate any

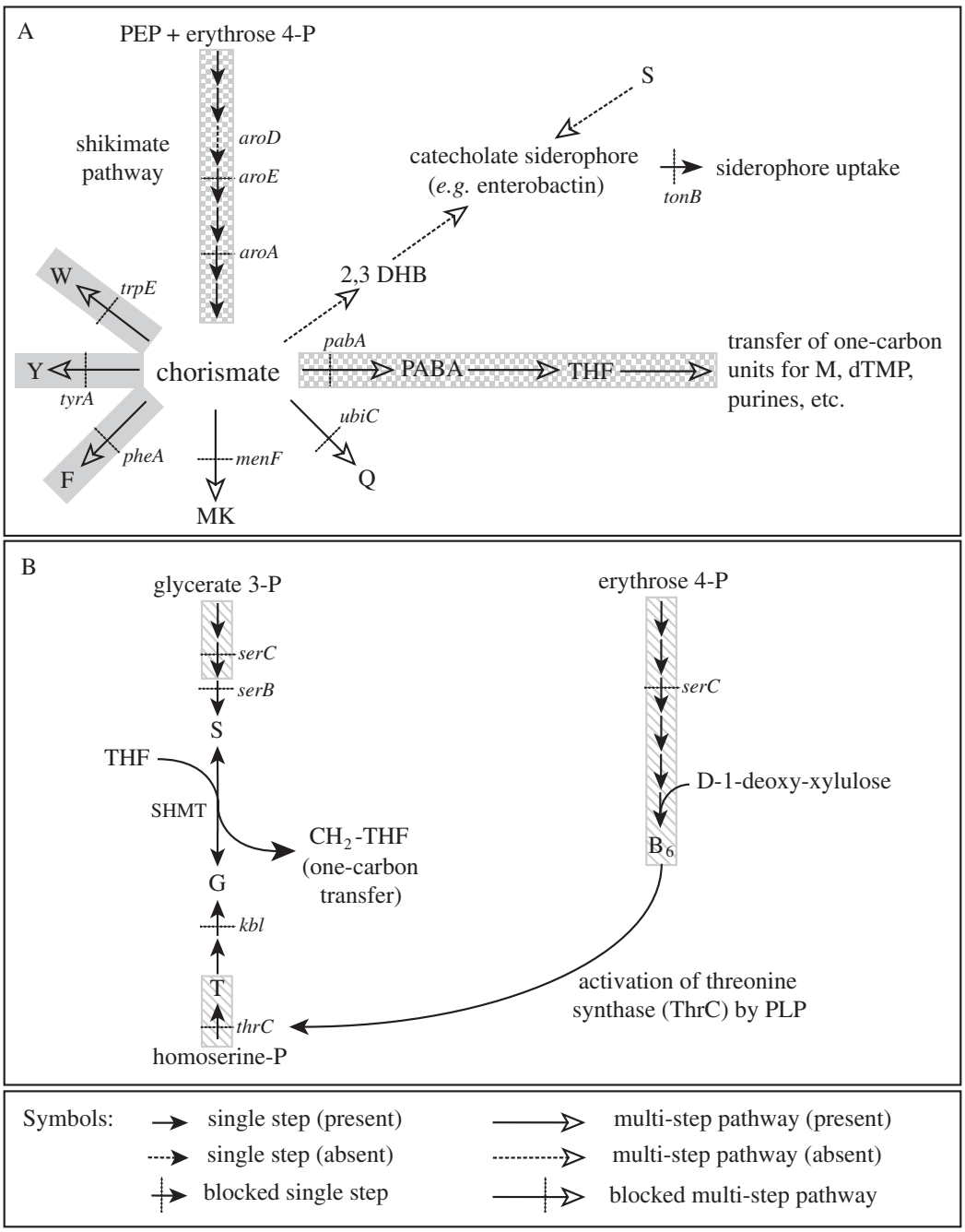

Fig. 2. Potential metabolic impact of mutations in *X. nematophila aroA* and *serC*. Putative *X. nematophila* biosynthetic pathways affected by mutation of (A) *aroA* or (B) *serC*. Rectangular boxes highlight the pathways in which metabolic blocks lead to class II (solid grey boxes), class III (checkered grey boxes) and class IV (hatched grey boxes) colonization defects and correspond to the patterns used on the histogram bars in Fig. 3.

Anticipated locations of metabolic blocks in mutants are indicated by cross-lines next to the name of the disrupted gene. Solid arrows indicate steps for which probable encoding genes were identified in the partial *X. nematophila* genome sequence.

A. A homologue of *aroD* encoding the enzyme catalysing the third step of the *E. coli* shikimate pathway was not detected in the genome. Production of chorismate via the shikimate pathway provides metabolic precursors for numerous other pathways. Genes predicted to encode synthetic functions for L-tryptophan (W), L-tyrosine (Y), L-phenylalanine (F), menaquinone (MK), ubiquinone (Q), para-aminobenzoate (PABA) and tetrahydrofolate (THF) were found in the *X. nematophila* genome. *X. nematophila* genes predicted to encode synthetic functions for 2,3-dihydroxybenzoate (2,3-DHB) or catecholate siderophores were not located.

B. The pathway on the left shows proposed metabolic steps involved in L-serine (S) biosynthesis. THF-dependent conversion of L-serine to glycine (G) by serine hydroxymethyltransferase (SHMT) serves as a source of one-carbon units, and is a potential link with THF metabolism depicted in A. The pathway on the right shows proposed metabolic steps involved in pyridoxine (B_6) biosynthesis. PEP, phosphoenolpyruvate; PABA, para-aminobenzoate; M, L-methionine; dTMP, deoxythymidine 5′-monophosphate; PLP, pyridoxal phosphate.

mutants specifically defective for only L-tyrosine or L-phenylalanine biosynthesis.

A separate screen of 2500 additional Tn*5* and Tn*10* mutants also yielded six mutants (0.24%) requiring either L-cysteine, L-methionine, L-threonine, L-histidine, L-leucine or the branched-chain amino acids L-valine and L-isoleucine. The Tn-disrupted genes in these mutants were determined to be *cysJ*, *pabA*, *thrC*, *hisB*, *leuB* and *ilvC* respectively (Table 1). Of note, HGB821, harbouring an insertion in *pabA*, is predicted to be disrupted for para-aminobenzoate, and therefore tetrahydrofolate, biosynthesis from chorismate (Fig. 2A). Disruption of this pathway is one possible cause of the IJ colonization defect exhibited by the *aroA* mutant. It is known in *E. coli* that tetrahydrofolate is required for L-methionine biosynthesis (Taylor and Weissbach, 1973), explaining the L-methionine auxotrophy associated with this strain. The *pabA* mutant grew in the absence of exogenous L-methionine only if para-aminobenzoate was provided (data not shown), demonstrating a functional link between para-aminobenzoate/tetrahydrofolate and L-methionine biosynthesis in *X. nematophila*. Furthermore, the *aroA* and *aroE* mutants also required either exogenous para-aminobenzoate or L-methionine for growth, validating the metabolic scheme depicted in Fig. 2A.

Finally, we also isolated 17 (0.5% of 3400 screened) *X. nematophila* Tn-mutants capable of growth in rich (LB) medium but incapable of growth on defined medium in the presence of all 20 L-amino acids. This class of mutants likely represents *X. nematophila* auxotrophs that are defective in other essential biosynthetic pathways (e.g. vitamins and nucleotides) that were not supplemented in our screening conditions. In a preliminary experiment to determine the growth requirements of some of these mutants, we found one, containing an insertion in *panB* (Table 1), that grew on defined medium in the presence of exogenous pantothenate and included this mutant in subsequent colonization experiments.

Based on the metabolic scheme depicted in Fig. 2, we also constructed targeted mutations in the remaining pathways that are derived from chorismate as well as in the last step of L-serine biosynthesis (encoded by *serB*). We made targeted deletions in the *X. nematophila* homologues of *tyrA-pheA* (these genes are directly adjacent in the *X. nematophila* genome), *ubiC*, *menF* and *serB* genes in order to generate mutants defective for L-tyrosine/L-phenylalanine, ubiquinone, menaquinone and L-serine biosynthesis respectively (Table 1, Fig. 2, *Experimental procedures*). In defined media experiments, the Δ*tyrA-pheA* and *serB* mutants required either both L-tyrosine and L-phenylalanine or L-serine respectively. To construct mutants deficient in biosynthesis of all three aromatic amino acids, we deleted the *tyrA-pheA* locus in the *trpE* strain background, creating a *trpE* Δ*tyrA-pheA* mutant (Table 1). This mutant required all three aromatic amino acids for growth on defined medium. The *ubiC* and *menF* mutants were not tested for auxotrophies on defined media, because the *aroA* mutant was previously determined to grow on defined medium in the absence of supplements to the ubiquinone and menaquinone biosynthetic pathways. This latter result may indicate that either *X. nematophila* synthesizes ubiquinone and menaquinone by a metabolic pathway other than that shown in Fig. 2 or that sufficient, contaminating amounts of these quinones exist in our defined medium preparation.

Because we failed to identify genes with potential catecholate/salicylate siderophore biosynthetic function in the *X. nematophila* genome, we chose to test the requirement for iron-acquisition in IJ colonization by disrupting a general component of the cell's ability to retrieve ferric-siderophores from the external environment. To accomplish this, we constructed a targeted deletion of *tonB*. In Gram-negative bacteria, the *tonB* product serves to couple energy derived via the proton-motive force to the transport of certain molecules from outer-membrane receptors, into the periplasm where they access cytosolic membrane transporters (Earhart, 1996; Postle and Kadner, 2003). Several classes of iron-chelating compounds (e.g. catecholate and hydroxamate siderophores and citrate), as well as coenzyme B_{12}, rely on TonB for entry into the cell. We therefore rationalized that constructing a *tonB* mutant should diminish cellular uptake of hypothetical ferric-siderophore(s) from the external environment. Of note, HGB965 (*tonB*) exhibits a slower growth rate *in vitro* than wild-type *X. nematophila* and hyper-secretes an iron-chelating substance on chrome-azurol S plates (Schwyn and Neilands, 1987) that likely reflects overproduction of the hydroxamate siderophore encoded in the genome (data not shown). Siderophore hyper-secretion is a commonly reported result of *tonB* disruption in other bacteria (Pugsley and Reeves, 1976; Thomas *et al*., 1999).

Colonization by metabolic mutants

Having isolated or constructed a number of defined metabolic mutants, we tested each of these strains for the ability to colonize the nematode intestine by evaluating the average number of viable bacteria associating with IJ populations (Fig. 3, *Experimental procedures*). Based on the colonization efficiencies of the mutants tested, we grouped them into four colonization classes. Class I includes mutants with lesions in *serB*, *hisB*, *cysJ*, *ilvC*, *ubiC*, *menF*, *panB and tonB*. These mutants colonize the IJ vesicle to wild-type levels suggesting that their respective metabolic requirements are satisfied by nutrients present within the host and therefore do not hinder their colonization abilities.

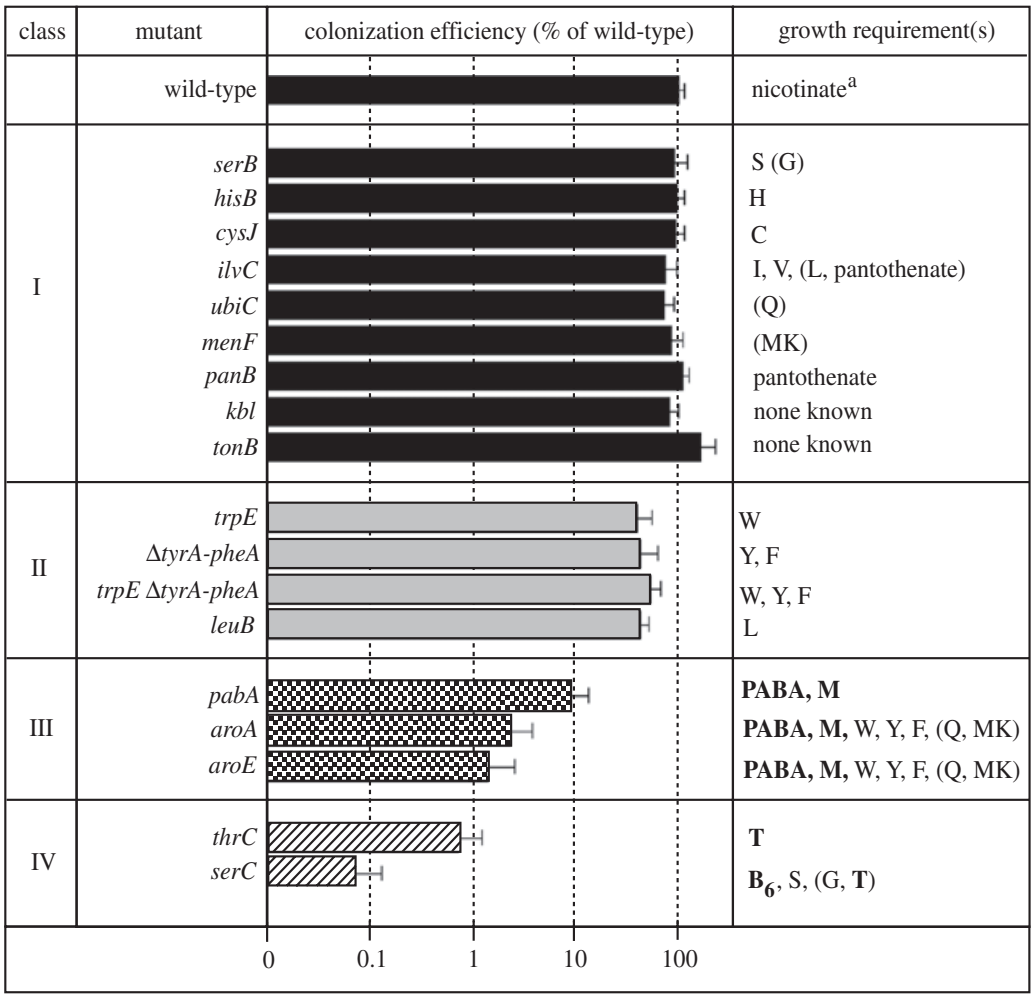

Fig. 3. Colonization by metabolic mutants. Mutants are grouped into four classes (I–IV) based on colonization efficiency and *in vivo* cell morphology (see text). Class I mutants (solid bars) exhibit wild-type colonization efficiency. Class II mutants (grey bars) exhibit moderately deficient colonization efficiency between 38% and 53% of wild-type. Class III mutants (checkered bars) share common defects in para-aminobenzoate (PABA), tetrahydrofolate (THF) and L-methionine (M) biosynthesis and exhibit colonization efficiency between 1% and 10% of wild-type. Class IV mutants (hatched bars) exhibit the lowest colonization efficiency (<1% of wild-type). Notes: [a]*X. nematophila* requires nicotinate. A requirement for this vitamin in other mutants listed is implied. Colonization efficiency is plotted on a log scale. The metabolic defects that are common among each member of class III and class IV mutants are in bold. Requirements given in parentheses are inferred from biosynthetic pathways that appear present in *X. nematophila* based on *in silico* analysis but which have not been established empirically. S, L-serine; G, glycine; H, L-histidine; C, L-cysteine; I, L-isoleucine; L, L-leucine; V, L-valine; Q, ubiquinone; MK, menaquinone; F, L-phenylalanine; Y, L-tyrosine; W, L-tryptophan; T, L-threonine; B_6, pyridoxine.

Class II includes *trpE*, *tyrA-pheA* and *leuB* mutants (Fig. 3). These mutants consistently exhibit moderately reduced colonization efficiency (38–53% of wild-type), suggesting that the metabolic defects associated with these mutants interfere with their ability to proliferate *in vivo*. IJs that emerged from lawns of the class II mutants *trpE*, Δ*tyrA-pheA* and *trpE* Δ*tyrA-pheA* contained rod-shaped bacteria that were morphologically similar to wild-type (data not shown). No attempt was made to genetically complement the colonization defect of any class II mutant.

Class III includes *aroA*, *aroE* and *pabA* mutants. These mutants exhibit >90% reduction in colonization efficiency (Fig. 3). Based on the metabolic scheme presented in Fig. 2A, these three mutants all share defects in para-aminobenzoate/tetrahydrofolate and L-methionine biosynthesis. The *pabA* mutant exhibits a three- to fivefold less severe colonization defect than *aroA* and *aroE* mutants, suggesting that the defects associated with *aroA* and *aroE* are caused by their combined para-aminobenzoate and aromatic amino acid requirements (Fig. 2A). Genetic complementation experiments established that colonization efficiency of the *pabA* mutant was increased to 110 ± 31% (average ± SD) of wild-type by addition of a single copy of the *X. nematophila pabA* gene *in trans*, establishing cau-

sality of this mutation to a decrease in IJ colonization (*Experimental procedures*).

Class IV mutants, *serC* and *thrC*, exhibit the most severe colonization defects of the metabolic mutants analysed in this study. *E. coli* threonine synthase, the product of *thrC* is a pyridoxyl-phosphate dependent enzyme and would be expected to have little activity in a pyridoxine (e.g. *serC*) auxotroph (Fig. 2). Therefore, a connection between the *serC* and *thrC* colonization defects likely lies in their shared inability to make L-threonine. Genetic complementation experiments established that colonization efficiency of the *thrC* mutant was increased to $77 \pm 4\%$ (average $\pm$ SD) of wild-type by addition of a single copy of the *X. nematophila thrABC* operon *in trans,* suggesting causality of this mutation to IJ colonization (*Experimental procedures*).

Threonine biosynthesis, but not catabolism is required for IJ colonization

The observed requirement for L-threonine biosynthesis (i.e. via threonine synthase) during IJ colonization led us to speculate that metabolism of nutrients through the threonine biosynthetic pathway to glycine, rather than biosynthesis of L-threonine itself, may be required (Fig. 2B). We therefore constructed a mutant with a defect in the putative *X. nematophila kbl-tdh* operon that is predicted to encode an NAD-dependent threonine dehydrogenase (*tdh*) and 2-amino-3-ketobutyrate coenzyme A ligase (*kbl*) (Reitzer, 1996). In *E. coli*, the combined effect of these two enzymes serves to degrade L-threonine to produce glycine and therefore provides the cell with an alternate pathway for glycine production (Reitzer, 1996). An *X. nematophila kbl* mutant did not exhibit decreased IJ colonization (Fig. 3), suggesting that L-threonine biosynthesis, but not catabolism to glycine via this route is required for IJ colonization.

Metabolic mutants exhibit aberrant colonization patterns in vivo

A reduced number of *X. nematophila* are isolated from nematodes grown on class II, III and IV metabolic mutants (Fig. 3, Heungens *et al*., 2002). This observation raises the possibility that these strains may either revert or acquire second-site suppressors that allow colonization of *S. carpocapsae*. To test this, we collected isolates of *aroA*, *aroE* and *serC* mutants that had successfully colonized IJs to low levels ('IJ-passaged' isolates) and evaluated their ability to colonize IJs in a subsequent experiment. If reversion or suppression had occurred, we expected the passaged strains to exhibit higher colonization than their unpassaged parents. However, we found that IJ-passaged isolates colonized the nematode intestine to similarly low levels as their un-passaged parent strains (data not shown), indicating that the partial colonization phenotype exhibited by these mutants is not caused by reversion or acquisition of suppressor mutations in these strains.

To assist in determining the location, morphology and distribution of colonizing metabolic mutant cells within the IJ intestine, we created *gfp*-labelled variants of several mutants (Table 1) and visualized their colonization behaviour using fluorescence microscopy. *S. carpocapsae* IJs were cultivated on *gfp*-labelled variants of wild-type *X. nematophila* or the *aroA*, *aroE*, *pabA*, *serC* and *thrC* metabolic mutants and allowed to emerge from culture plates on their own (mature IJs) as previously described (Martens *et al*., 2003a).

Bacteria observed within IJs that emerged from culture with the metabolic mutants tested exhibited two new colonization phenotypes that differed from the colonization behaviour exhibited by wild-type *X. nematophila* (Fig. 4). First, many IJs grown on lawns of each of the mutants (*aroA*, *aroE*, *pabA*, *serC* and *thrC*) contained several small, spherical, *gfp*-positive signals in the intestinal vesicle (e.g. Fig. 4E–G). These *gfp*-positive spheres are similar in size to single, wild-type cells that have been converted to spheroplasts by treatment with sucrose and lysozyme (Fig. 4H), suggesting that they represent individual *X. nematophila* cells that had converted to a spherical morphology.

Second, some IJs grown on a subset of the mutants tested (*aroA*, *aroE* and *pabA*) contained sparse growth of filamentous cells in the vesicle (Fig. 4C–E). This growth behaviour was not observed with mutants in *serC* or *thrC*, but is shared by mutants with a common requirement for para-aminobenzoate. Stationary-phase (16 h) cultures of the *aroA*/*gfp*$^+$ mutant, grown *in vitro* in LB medium, exhibited a similar morphology as wild-type cells (Fig. 4I), demonstrating that the filamentous morphology does not occur in this growth condition but does occur during growth *in vivo* (data not shown). The sparse colonization phenotype exhibited by these mutants resembles that of wild-type *X. nematophila* in immature (oligo-colonized) IJs harvested prior to outgrowth of the bacterial population (Martens *et al*., 2003a). However, wild-type bacteria in immature IJs do not exhibit filamentous morphology and in *aroA*-, *aroE*- or *pabA*-derived nematodes this oligo-colonized state persists for several weeks after IJs form, suggesting that these filamentous bacteria either are growing slowly or have prematurely arrested growth. Of note, some IJs containing filamentous mutant cells also contained spherical cells demonstrating that these two morphologies can be present in the same vesicle (e.g. Fig. 4E shows a vesicle containing both filamentous and spherical *pabA* cells).

Next, we evaluated the behaviour of colonizing bacteria exhibiting the spherical cell (Fig. 4E–G) and filamentous-

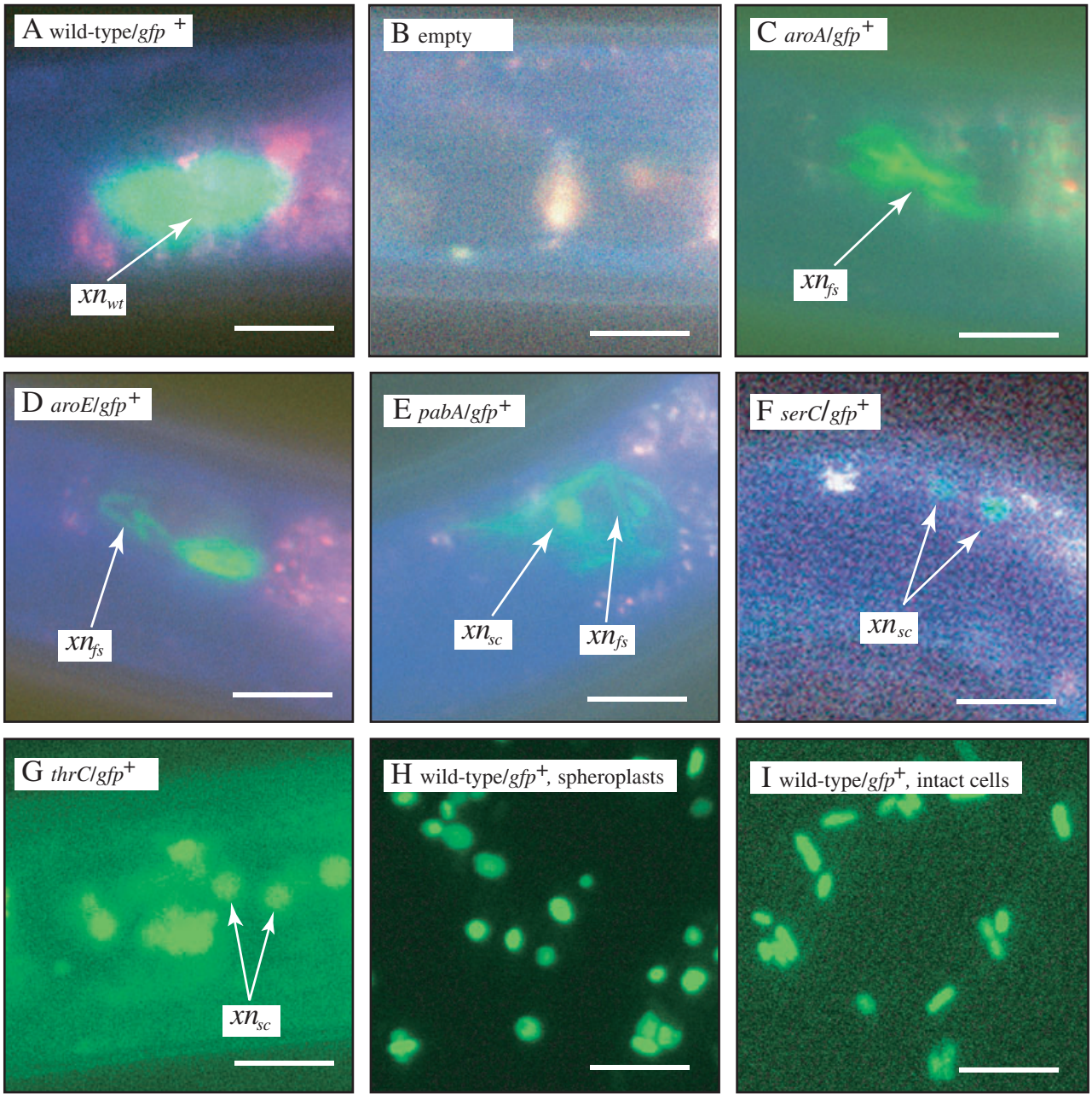

Fig. 4. Mutant colonization phenotypes *in vivo*. IJs grown on *gfp*-labelled variants of several colonization-deficient auxotrophs were analysed by fluorescence microscopy to determine the location and number of mutant *X. nematophila* within their vesicles.
A. Vesicle of an IJ grown on wild-type/*gfp*$^+$. The vesicle contains a tightly packed cluster of wild-type/*gfp*$^+$ (xn_{wt}, ~50 cfu per IJ on the average), although individual cells cannot be seen in this example.
B. An uncolonized IJ with an empty vesicle for comparison to other panels.
C. Vesicle of an IJ grown on *aroA*/*gfp*$^+$ showing filamentous bacterial cells (xn_{fs}) in the vesicle.
D. Vesicle of an IJ grown on *aroE*/*gfp*$^+$, containing filamentous cells (xn_{fs}) similar to *aroA*/*gfp*$^+$.
E. Vesicle of an IJ grown on *pabA*/*gfp*$^+$, containing numerous filamentous cells (xn_{fs}) and one spherical cell (xn_{sc}).
F. Vesicle of an IJ grown on *serC*/*gfp*$^+$ containing two spherical *X. nematophila* cells (xn_{sc}).
G. Vesicle of an IJ grown on *thrC*/*gfp*$^+$ containing numerous spherical cells (xn_{sc}).
H. Wild-type/*gfp*$^+$ treated with lysozyme/sucrose/EDTA to create spheroplasts (*Experimental procedures*). Note the similar size and shape of these spheroplasts generated *in vitro* to the spherical cells in E, F and G.
I. HGB338 (wild-type/*gfp*$^+$) cells taken directly from a stationary-phase LB culture showing the characteristic rod-shape of wild-type *X. nematophila*.
Magnification is ×600; bars = 5 μm.

sparse (Fig. 4C–E) phenotypes over time. To accomplish this we analysed IJs grown on lawns of wild-type/*gfp*$^+$, *serC*/*gfp*$^+$ and *aroA*/*gfp*$^+$ using fluorescence microscopy over a time course of ~6 weeks. IJs were evaluated by epifluorescence microscopy immediately after emerging from culture and then at subsequent 7 day intervals until a maximum of 41 days post emergence (Fig. 5). At each time point, 200 IJs grown on each strain were scored for the presence of the following phenotypes: >1/3 fully colonized (e.g. Fig. 4A), empty (e.g. Fig. 4B), <1/3 fully colonized (this colonization state includes the filamentous-sparse phenotype; e.g. Fig. 4C–E) or spherical cell (e.g. Fig. 4E–G). Additionally, the average number of viable bacteria associated with a population of 10^4 IJs was evaluated at each time point ('gross assay', *Experimental procedures*).

As expected, IJs emerging from control lawns inoculated with wild-type/*gfp*$^+$ were fully colonized even at 1 day post emergence as evaluated both by microscopic evaluation and gross assay (Fig. 5A). Over the time course, the number of individual IJs microscopically observed to be colonized by wild-type/*gfp*$^+$ remained constant (~90%). Similarly, viable counts of wild-type/*gfp*$^+$ associated with this IJ population also remained nearly constant over time with a substantial decline in viable cfu per IJ occurring only at 41 days post emergence (Fig. 5 legend) likely attributed to an observed decrease in IJ viability during prolonged storage (data not shown).

Over the time course, IJs colonized by *serC*/*gfp*$^+$ exhibited low (0.2% of wild-type), but stable colonization efficiency of $0.16 \pm 0.04\%$ (average $\pm$ SD) (Fig. 5B). Only one out of 1200 (0.08%) IJs grown on this mutant was observed to have a full vesicle (similar to Fig. 4A). Although this sample number is small, a colonization frequency of 0.08% of the total IJs observed by microscopy is similar to the 0.16% colonization efficiency determined by viable count, suggesting that partial colonization of IJs by the *serC*/*gfp*$^+$ mutant is such that very few individual IJs (<1 in 10^3) retain a full/nearly full intestinal population of this mutant. The percentage of IJs carrying *serC*/*gfp*$^+$ spherical cells decreased from 75% to 7% over the time course, without a detectable decline in viable cfu per IJ. This decrease was accompanied by a concomitant increase in the frequency of empty vesicles (Fig. 5B). The sharp decline in the percentage of IJs containing spherical cells over time is a characteristic feature of colonization by *serC*/*gfp*$^+$ (Fig. 5B) and was observed in a separate experiment over a similar time course (data not shown). This decline is consistent with the hypothesis that these spherical cells have been retained in the IJ vesicle, but do not contribute to the viable population. Because the spherical cell phenotype is lost over time without a concomitant decrease in viable bacterial numbers, we conclude that it represents the outcome of a non-productive or abortive

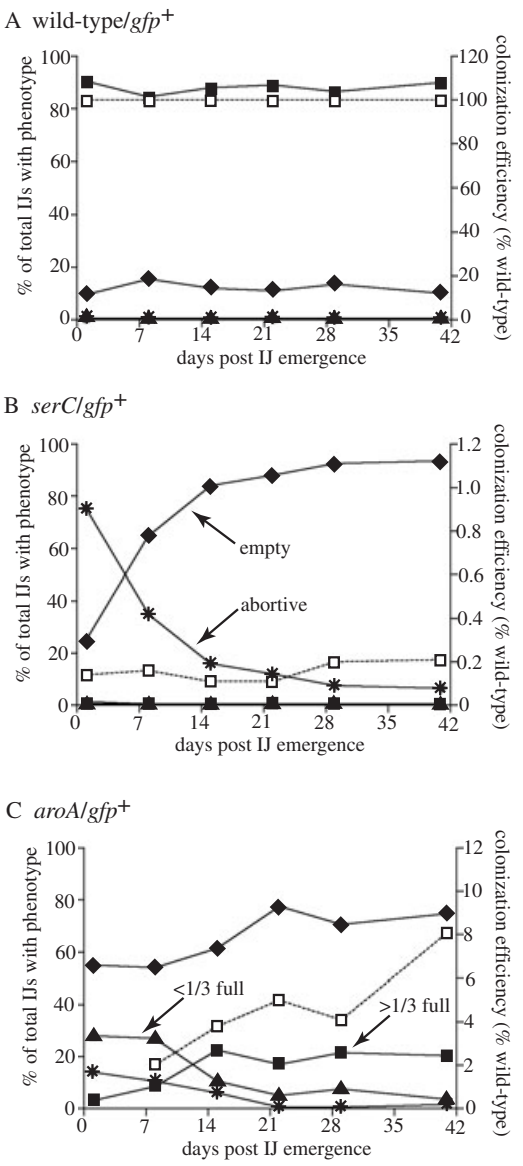

Fig. 5. Mutant colonization phenotypes over time. IJs that had emerged from lawns of (A) wild-type/*gfp*$^+$, (B) *serC*/*gfp*$^+$ or (C) *aroA*/*gfp*$^+$ were examined over a time course ending 41 days post emergence. At each time point, the percentage of IJs exhibiting each of four colonization phenotypes was scored ($n = 200$ for each time point, plotted on left axis). Phenotypes scored were: vesicles with >1/3 full capacity of *X. nematophila* (e.g. Fig. 4A) (solid squares), empty vesicles (e.g. Fig. 4B) (solid diamonds), vesicles with <1/3 full capacity of *X. nematophila*, including filamentous cells (e.g. Fig. 4C–E) (solid triangles) and vesicles containing spherical (abortive) cells (Fig. 4F–G) (asterisks). In cases where a single IJ cultivated on *aroA*/*gfp*$^+$ contained bacteria exhibiting both filamentous and spherical cells (similar to Fig. 4E) the specimen was counted twice and scored once for each phenotype (although such IJs accounted for <1% of total IJs counted). The average number of viable *X. nematophila* recovered (by sonication and plating) from 10^4 IJs was also determined at each time point for each IJ population (open squares with dashed line, plotted on right axis). For wild-type/*gfp*$^+$-grown IJs, the actual average numbers of viable cfu per IJ were determined to be 56, 51, 47, 56, 46 and 31 at day 1, 8, 15, 22, 29 and 41 post emergence respectively. For calculation of mutant colonization efficiencies at each time point, each of these values was set as 100% colonization.

colonization event prompting us to term the spherical cell phenotype 'abortive' colonization.

Phenotypes observed in IJs colonized by *aroA*/*gfp*$^+$ were dynamic over the time course (Fig. 5C), although only one such experiment was conducted and therefore the reproducibility of phenotypic trends was not verified. At early times post emergence, this strain exhibited a higher frequency of filamentous-sparse colonization (i.e. <1/3 full vesicle) compared with that at later time points. Conversely, the proportion of IJs observed to be highly colonized (>1/3 full vesicle) was initially lower at early time points and increased over time, suggesting that this mutant increases colonization density slowly over time. The frequency of the spherical cell phenotype in IJs colonized by the *aroA*/*gfp*$^+$ mutant also decreased over time. The magnitude of this change over time was not as striking as with *serC*/*gfp*$^+$ owing to the fact that there were initially fewer IJs containing abortive events (14% at 1 day post emergence).

Abortive phenotype in other colonization mutants

Thus far, we had observed the abortive (i.e. spherical cell) colonization phenotype in the metabolic mutants *aroA*, *aroE*, *pabA*, *serC* and *thrC*. To determine if this phenomenon also occurs with other known colonization-defective mutants we constructed *gfp*-labelled derivatives of the class II metabolic mutants *trpE*, Δ*tyrA-pheA* and *trpE* Δ*tyrA-pheA* (Table 2). We also constructed *gfp*-labelled derivatives of five other previously reported *X. nematophila* colonization-deficient mutants: *rpoS*, *nilA*, *nilB*, *nilD* and *iscA*::Tn*10*::*hscB* (Table 1) (Vivas and Goodrich-Blair, 2001; Heungens *et al*., 2002; Martens *et al*., 2003b).

Infective juveniles were grown on each of these *gfp*-labelled strains and analysed to determine if they contained abortive colonization events. We quantitatively scored IJs emerging from individual cultures containing 11 of the 13 *gfp*-labelled mutants (all except *thrC* and *pabA*, which were scored qualitatively) for the presence of abortive *X. nematophila* cells in the IJ vesicles (Table 2). The class II mutants *trpE*, Δ*tyrA-pheA* and *trpE* Δ*tyrA-pheA* exhibited a low rate of abortive colonization (3–11%). As noted above, the *thrC* and *pabA* mutants also displayed abortive colonization, with *thrC* being highly abortive (Table 2, Fig. 4G) and *pabA* exhibiting both abortive colonization and the filamentous-sparse phenotype, similar to *aroA* and *aroE* (Fig. 4E).

In contrast to the class II, III and IV metabolic mutants, none of the other mutants analysed exhibited the abortive colonization phenotype (Table 2), suggesting that the abortive phenotype is characteristic of only a subset of colonization deficient mutants and is related to certain auxotrophies.

Discussion

For mutualistic *X. nematophila* to colonize and proliferate within the intestinal vesicle of *S. carpocapsae*, it must be able to access sufficient nutrients while present within this

Table 2. Observation of abortive phenotype in *gfp*-labelled colonization mutants.

gfp-labelled strain[a]	Relevant defect[b]	Mutant class[c]	Abortive colonization[d]
Wild-type	None	NA	No (<0.2)
Abortive			
serC	B_6 auxotroph	IV	Yes (57%)
thrC	T auxotroph	IV	Yes (ND)
pabA	PABA, M auxotroph	III	Yes (ND)
aroA	W, Y, F, Q, MK, PABA, M auxotroph	III	Yes (19%)
aroE	W, Y, F, Q, MK, PABA, M auxotroph	III	Yes (5%)
trpE	W auxotroph	II	Yes (3%)
Δ*tyrA-pheA*	Y, F auxotroph	II	Yes (5%)
trpE Δ*tyrA-pheA*	W, Y, F auxotroph	II	Yes (11%)
Non-abortive			
rpoS	Transcriptional regulator	NA	No (<0.2)
nilA	Unknown	NA	No (<0.2)
nilB	Putative outer membrane protein	NA	No (<0.2)
nilD	Putative small RNA	NA	No (<0.2)
iscRSUA::Tn*10*::*hscBA*	Iron-sulphur cluster formation	NA	No (<0.2)

a. See Table 1 and *Experimental procedures* for description of *gfp*-labelled strain construction.
b. Growth requirements associated with metabolic mutants are abbreviated as described for Fig. 2.
c. NA indicates strains (wild-type and mutants) that do not belong to any of the four colonization classes summarized in Fig. 3.
d. IJs grown on each *gfp*-labelled strain were scored between 2 d and 4 days post emergence from lipid-agar (LA) culture. Five hundred IJs were scored for each strain (limit of detection of 0.2%) with the exception of *thrC* and *pabA,* for which several dozen IJs were observed qualitatively. The percentage of IJs containing abortive *X. nematophila* are given in parentheses. For IJ populations within which abortive colonization was not observed, the abortive rate is given as the limit of detection (<0.2), however, abortive colonization was never observed in these populations. ND indicates that abortive colonization was not quantified.

host niche. With this study, we report detailed investigation of the colonization abilities of a number of *X. nematophila* metabolic mutants (Figs 3–5). Our findings provide insight into the nature of the nutrient sources that *X. nematophila* may access from non-*de novo* sources during growth *in vivo* (several amino acids and vitamins), as well as identify nutrients (para-aminobenzoate, pyridoxine and L-threonine) that are likely insufficiently available or accessible as supplements for normal bacterial growth *in vivo*. Observations of the abortive and filamentous colonization phenotypes raise new hypotheses regarding the *X. nematophila* nematode-colonization process. These include the possibility that some colonization mutants are retained in the vesicle but subsequently fail to grow normally (abortive mutants) whereas others are deficient in colonization steps preceding retention in the vesicle (non-abortive mutants).

Abortive colonization of the vesicle

Eight of the *X. nematophila* mutants characterized in this study exhibit abortive colonization typified by formation of a spherical cell morphology *in vivo* (Table 2). Decreasing numbers of IJs colonized by spherical cells over time correlate with increasing numbers of empty IJs (Fig. 5B), leading us to conclude that abortive *X. nematophila* are non-viable and lost from the IJ population over time. Wild-type *X. nematophila* has been observed to spontaneously adopt this spherical cell morphology under a variety of other conditions including during release from IJs stimulated with insect haemolymph and during stationary-phase culture in LB culture (E.C. Martens and H. Goodrich-Blair, unpublished data). Another group recently reported that a proportion of *X. nematophila* cells within infected insects also take on a spherical shape (Sicard *et al*., 2004b). The significance, if any, of this spherical morphology to *X. nematophila* biology is uncertain, but the fact that it occurs in a variety of growth conditions implies that it might be a behaviour intrinsic to *X. nematophila* (e.g. autolysis) and not a response to one particular environment. Approximately 10% of IJs emerging from wild-type *X. nematophila* lawns are uncolonized, and it is possible that these are the result of an abortive colonization process. However, if so, one would expect some fraction of these to exhibit the presence of abortive cells. At 1 day post emergence, we observed ~75% and ~15% abortive colonization rates in *serC*- and *aroA*-grown IJs respectively. Using these values, if abortive colonization occurs in wild-type colonized IJs, we would expect to observe 3–15 abortive events (15–75% of the 20 uncolonized IJs observed). However, at 1 day post emergence, no abortive events were observed in IJs derived from wild-type lawns. In fact, this phenomenon has not been noted in many similar experiments (not shown) increasing the sample size, and further supporting that uncolonized IJs from wild-type lawns are not the result of an abortive process.

The observation that some *X. nematophila* colonization-deficient mutants are abortive, while others are not (Table 2) is noteworthy. Classification of colonization mutants as abortive or non-abortive helps differentiate these mutants into functionally distinct classes. Adherence of microorganisms to host tissues is often an important first step in the process of host colonization (Hultgren *et al*., 1996). Therefore, nematode colonization initiation may be attributed to specific adherence of *X. nematophila* within this host niche. Of note, we have found that both abortive and filamentous *X. nematophila* cells (Fig. 4) associate with a defined structure, the intravesicular structure (IVS), which occurs within the lumen of the IJ intestine (E.C. Martens and H. Goodrich-Blair, 2005). Thus, if adherence of *X. nematophila* to the IVS is a step towards colonization initiation, colonization mutants that do not exhibit abortive behaviour may be blocked prior to this adherence event while abortive mutants are blocked in an event subsequent to interaction with the IVS (i.e. during *in vivo* growth).

Non-de novo *nutrients are available to* X. nematophila *in vivo*

Xenorhabdus nematophila class I mutants in *serB*, *hisB*, *cysJ*, *ilvC*, *ubiC*, *menF*, *panB*, *kbl* and *tonB* exhibit normal IJ colonization efficiency (Fig. 3). As some of these mutants exhibit defined growth requirements *in vitro* (i.e. L-serine, L-histidine, L-cysteine, L-isoleucine, L-valine and pantothenate), we conclude that during growth within the IJ vesicle *X. nematophila* has access to sufficient quantities of these nutrients from non-*de novo* sources. Additionally, *X. nematophila* may not rely on TonB-mediated uptake of external compounds such as ferric-siderophores or coenzyme B_{12} during IJ colonization.

The class II mutants in *trpE*, *tyrA-pheA* and *leuB* display moderate reductions in colonization efficiency relative to wild-type and class I mutants (Fig. 3). The amino acids for which these strains are auxotrophs, L-tryptophan, L-tyrosine, L-phenylalanine and L-leucine may be limiting during bacterial growth in the vesicle, although enough of each of these nutrients must be accessible to allow ~50% colonization efficiency. Of note, the *leuB* mutant exhibits reduced colonization, while the *ilvC* mutant does not. Although the position of the *ilvC* biosynthetic block should disrupt the ability to synthesize L-leucine *de novo* from central metabolites such as pyruvate (Umbarger, 1996), when the *ilvC* mutant is grown on defined medium containing L-valine it does not show a requirement for L-leucine (data not shown). This result is consistent with findings in *E. coli* and *Sa. enterica* that transaminases B

and C can deaminate L-valine to produce 2-ketoisovalerate (Whalen and Berg, 1982), a precursor for L-leucine and pantothenate biosynthesis (Umbarger, 1996). Thus, the *ilvC* mutant likely acquires sufficient non-*de novo* L-valine *in vivo* to satisfy its L-valine, L-leucine and pantothenate requirements. Genetic complementation experiments that test the causality of the reported gene disruptions in the class II mutants will be required to establish that the lower colonization efficiencies of these mutants are attributable to their respective mutations.

The source of non-*de novo* amino acids and the form in which they are present for *X. nematophila* remains unclear. At least three possibilities exist: (i) amino acids are nematode-derived and present in free amino acid form; (ii) amino acids are nematode-derived and present in peptide form, perhaps as components of secreted mucins or host cell-surface proteins; and (iii) amino acids are bacteria-derived from a stored source that was accumulated prior to colonization of the IJ vesicle. Consistent with the first two possibilities, it is worthwhile to note that *S. carpocapsae* IJs that are uncolonized survive longer than those colonized by *X. nematophila* (Mitani *et al*., 2004), supporting the idea that the non-feeding IJ contributes some of its own stored nutrients to foster bacterial growth.

The concept of mutualistic bacteria obtaining nutrients from their host in the form of free or peptide amino acids has precedent in other models of microbe–host colonization (Graf and Ruby, 1998; Ferraioli *et al*., 2002). For example, the lumen of the *Euprymna scolopes* squid light organ, within which the bacterial mutualist *Vibrio fisheri* grows, contains amino acids in both the free and peptide forms (Graf and Ruby, 1998). A similar host-derived source of amino acids could be available to *X. nematophila*. Electron microscopy of both colonized and uncolonized *Steinernema* spp. revealed what appeared to be a polymeric matrix (possibly mucus) in the lumen of the IJ vesicle (Bird and Akhurst, 1983), and *X. nematophila* may utilize amino acids and carbohydrates present in host mucus during *in vivo* growth. If this hypothesis is true, then one would anticipate that these bacteria may enzymatically degrade this substance(s) to prepare its components for uptake and subsequent catabolism. Future analysis of the *X. nematophila* genome (http://xenorhabdus.danforthcenter.org) should provide insight into the potential repertoire of amino acid and peptide permeases, as well as degradative and catabolic functions that may serve these roles, thus allowing the hypothesis that *X. nematophila* degrades host mucins to be tested.

The third potential source of non-*de novo* amino acids during *X. nematophila* growth *in vivo* is from within the colonizing bacteria themselves such as through the accumulation of intracellular crystalline protein inclusions (Couche and Gregson, 1987; Couche *et al*., 1987). Accumulation of inclusions by *X. nematophila* prior to gaining access to the IJ vesicle may represent a mechanism for this species to store amino acids prior to colonization (i.e. inside an insect cadaver) that could later serve as a nutrient source inside the nematode. Evidence against this hypothesis comes from the conflicting observations that L-threonine is abundant in *X. nematophila* crystalline inclusions (Couche and Gregson, 1987) but the *thrC* mutant reported here is deficient for colonization (Fig. 3), suggesting it does not encounter/or store sufficient L-threonine to promote *in vivo* growth.

Some nutrients are not available from non-de novo *sources* in vivo

The colonization deficiencies associated with the class III and class IV mutants (Fig. 3) suggest that during growth *in vivo* these mutants fail to access sufficient amounts of the nutrients that they require. It is unlikely that the metabolic blocks associated with any of these mutants result in the accumulation of toxic biosynthetic intermediates because these mutants grow well *in vitro* on both LB (Heungens *et al*., 2002 and data not shown) and defined medium containing the appropriate supplements (data not shown).

We conclude that the colonization defects associated with the class III *aroA*, *aroE* and *pabA* mutants result from their common requirements for para-aminobenzoate, L-methionine and/or potentially other undetermined nutrients. The *aroA* and *aroE* mutants exhibit consistently lower colonization efficiencies relative to *pabA* (three- to fivefold, Fig. 3), and this may be attributed to their additional defects in aromatic amino acid biosynthesis (similar to the class II mutants with aromatic amino acid requirements). Several para-aminobenzoate-dependent metabolic functions are known in *E. coli* and are attributed to a lack of tetrahydrofolate biosynthesis (Fig. 2) (Matthews, 1996). These include synthesis of L-methionine, glycine, purine, pantothenate, thymidylate and Met-tRNA^{fMet} as well as catabolism of glycine by the glycine-cleavage pathway. In this work, only L-methionine biosynthesis was shown empirically to be affected in para-aminobenzoate mutants and L-methionine biosynthesis was not specifically shown to be the para-aminobenzoate-dependent product required for colonization. The question of which para-aminobenzoate-dependent function(s) is required by *X. nematophila* for normal growth *in vivo* will need to be addressed experimentally by construction of additional mutants in tetrahydrofolate-dependent pathways.

The class III mutants do not populate the vesicle to similar density as wild-type *X. nematophila*. Rather, they appear to be 'trapped' in the growth stage of colonization;

after they have been retained in the vesicle, but before they fully populate this niche. Similar to abortive cells, filamentous *aroA* and *aroE* cells have been observed to colocalize with the *S. carpocapsae* IVS (E.C. Martens and H. Goodrich-Blair, 2005), suggesting that nematode colonization may occur through bacterial adherence to this structure.

The defects associated with the class IV *serC* and *thrC* mutants likely result from their respective requirements for pyridoxine and L-threonine (Fig. 2B). Comparison of the *serC* mutant with the class I *serB* mutant (Fig. 3) clearly shows that L-serine auxotrophy is not the cause of the colonization defect associated with *serC*. Pyridoxine production via SerC, or another defect associated with this mutant, is therefore the likely cause of its colonization deficiency.

Mutants in *serC* and *thrC* exhibit the most severe nematode-colonization defects of the mutants discussed in this report (<1% wild-type colonization efficiency) (Figs 1 and 3). In contrast to their low colonization efficiencies, the *serC* and *thrC* mutants display the highest frequencies of abortive colonization (Fig. 5B and Table 2), supporting the hypothesis that effective IJ colonization and abortive colonization occur to the exclusion of one another. In newly emergent IJs grown on the *serC* mutant as many as 75% of individuals are abortively colonized (Fig. 5B). The rate of abortive colonization with the *thrC* mutant has not yet been quantified, but all IJs grown on this mutant that have been observed so far only contain abortive *X. nematophila* (Fig. 4G). The abortive phenotypes of the *serC* and *thrC* mutants are not identical. IJs containing abortive *serC* cells have not been observed to contain more than four individual spherical cells (data not shown), whereas IJs containing abortive *thrC* cells typically contain many (>4) abortive spherical cells (e.g. Fig. 4G). Thus, it appears that the *thrC* mutant may abort growth at a later time after colonization initiation than *serC*, allowing more cells to accumulate in the vesicle. This suggests that L-threonine is not the only nutrient for which the *serC* mutant is lacking *in vivo*, but that other pyridoxine-dependent nutrients are also lacking, causing this mutant to abort colonization more rapidly than *thrC*.

The specific requirement for bacterial *de novo* synthesis of L-threonine, but not other amino acids, in the IJ vesicle may be consistent with the hypothesis that *X. nematophila* accesses nutrients contained in host mucins during *in vivo* growth. Because host mucins are frequently O-glycosylated on L-serine and L-threonine residues (Hanisch, 2001), it is possible that *X. nematophila* has access to O-glycosylated L-threonine but lacks the enzymatic capacity to catabolize it to useable L-threonine. If so, then an inability to catabolize O-glycosylated residues must not extend to L-serine, because this amino acid is available non-*de novo* in the IJ vesicle.

Concluding remarks

The analysis of *X. nematophila* metabolic mutants in this report provides a glimpse of the host niche in which these bacteria multiply during nematode colonization. Although several nutrients essential for bacterial growth are limiting or unaccessible within the IJ vesicle, this environment is replete with respect to a number of non-*de novo* amino acids and vitamins. Future experiments that investigate the chemical source(s) of nutrients that fuel *X. nematophila* growth *in vivo* should clarify how this bacterium has specifically adapted to existence within the intestine of *S. carpocapsae*.

Experimental procedures

Strains, plasmids and culture conditions

Bacterial strains and plasmids are listed in Table 1. Permanent stocks of bacterial strains were maintained at −80°C in LB medium (Miller, 1972) supplemented with 25% glycerol (for *E. coli*) or 10% dimethyl sulfoxide (for *X. nematophila*). Unless stated otherwise, *X. nematophila* and *E. coli* were grown at 30°C in/on LB medium that had either not been exposed to light or to which 0.1% pyruvate had been added (Xu and Hurlbert, 1990). When appropriate, media were supplemented with chloramphenicol (30 μg ml^{-1}), streptomycin (25 μg ml^{-1}), rifampicin (100 μg ml^{-1}), erythromycin (200 μg ml^{-1}), kanamycin (50 μg ml^{-1}), sucrose (5% w/v) and agar (15 g l^{-1}). Defined medium for *X. nematophila* and solid, lipid-agar (LA) medium for coculture of *S. carpocapsae* on lawns of *X. nematophila* were prepared as previously described (Wouts, 1981; Vivas and Goodrich-Blair, 2001; Orchard and Goodrich-Blair, 2004). *E. coli* S17-1 λ *pir* (Simon *et al.*, 1983) was used to conjugally transfer plasmids into *X. nematophila* (Forst and Tabatabai, 1997). *S. carpocapsae* was maintained and cultured *in vivo* as described (Vivas and Goodrich-Blair, 2001; Martens *et al.*, 2003a). IJ stocks for general nematode maintenance or time-course experiments were stored in a thin (~0.5 cm depth) layer of distilled water in tissue culture flasks at room temperature and in the dark.

For construction of Tn*10*-kan donor plasmid pSAG1, a 4.8 kb EcoRI fragment was removed from construct λ1316 (Kleckner *et al.*, 1991) and ligated into suicide vector pR6Kcam that was also digested with EcoRI. pR6Kcam is a derivative of plasmid pGP704 (Miller and Mekalanos, 1988) that was digested with PstI to remove a segment of the *bla* gene and then ligated with the *cat* gene from pBCSK+/– (Stratagene, La Jolla, CA) that had been PCR-amplified with PstI ends. To construct plasmid pDel-1KS, plasmid pECM20 (Martens *et al.*, 2003a) was digested with PstI, restriction ends blunted with mung bean nuclease, digested again with XbaI and ligated to a 2.893 kb XbaI-EcoRV fragment from plasmid pRES1 that contains *sacB-aphA*. DNA fragments used for mutagenesis were cloned into unique XbaI and EcoRV sites of pDel-1KS. Plasmid pKR100B-Str was constructed by digesting pKR100B (Martens *et al.*, 2003a) with SalI and PstI to remove the *cat* gene and the backbone vector was ligated to a ~2.1 kb Str^r cassette excised from pHRP317 (Parales and Harwood, 1993). *gfp*-labelling plasmid pECM21

was constructed by digesting pECM20 (Martens *et al*., 2003a) with PstI to remove the *cat* gene, blunting the ends with mung bean nuclease and ligating the backbone vector to the *aphA* gene amplified from Tn*903* with blunt ends (Kleckner *et al*., 1991). The orientation of *aphA* in this construct was not determined. To label *X. nematophila* strains with *gfp*, either pECM20 or pECM21 was conjugated into recipient strains from *E. coli* S17-1 λ *pir* and exconjugants were selected on either chloramphenicol or kanamycin as appropriate. Candidate *gfp*$^+$ strains were evaluated by fluorescence microscopy to verify *gfp* expression.

Complementation of mutant strains

Select mutants were genetically complemented using a single copy of the gene or operon that was determined to be disrupted in each mutant. Complementing genes were delivered to the *X. nematophila att* Tn*7* site (Martens *et al*., 2003c) using the Tn*7* vector pEVS107 (McCann *et al*., 2003) (Table 1). Fragments containing genes for complementation, as well as >500 bp of the region lying upstream of each gene or operon, were amplified from HGB081 using the primers listed in Table S1. Fragment ends were digested with appropriate restriction enzymes and subsequently cloned into corresponding restriction sites in pEVS107. Insertions of Tn*7* constructs into *X. nematophila att* Tn*7* were verified as described previously (Cowles and Goodrich-Blair, 2004).

For complementation of HGB316 (*serC*) with *serC* only, a pEVS107-based construct carrying the entire *serC-aroA* locus was digested with KpnI (which cleaves downstream of *aroA* in the pEVS107 polylinker), the restriction ends were blunted by treatment with mung bean nuclease, the plasmid was digested again with HpaI (which cleaves in the *serC-aroA* intergenic region) to remove all of the *aroA* gene and finally religated.

Infective juvenile colonization assay by viable count (gross assay)

The abilities of wild-type and mutant derivatives of *X. nematophila* to colonize the *S. carpocapsae* IJ vesicle were determined as previously reported (Martens *et al*., 2003a). However, here we report *X. nematophila* colonization as 'colonization efficiency' rather than average cfu per IJ. Colonization efficiency is defined as the percentage of wild-type colonization exhibited by mutant strains and therefore equals 100 × [(avg. mutant cfu per IJ)/(avg. wild-type cfu per IJ)]. All colonization efficiency data shown, with the exception of those in Fig. 5, are the average of three or more replicate colonization assays and are provided as average ± SD.

gfp-*labelled strains and fluorescent microscopy*

Infective juveniles grown on *gfp*-labelled strains were prepared for microscopy as previously described for *S. carpocapsae* (Martens *et al*., 2003a), except that levamisole (Sigma, St. Louis, MO), instead of sodium azide, was added at a concentration of 1 mg ml^{-1} to 2% agarose as a paralisant. Microscopy was performed on a Nikon Eclipse TE300 inverted microscope. Fluorescence microscopy of green fluorescent protein-containing samples was performed using FITC, TRITC and triple-band DAPI/FITC/TRITC filter sets (Chroma, Brattleboro, VT; items #31001, #31002 and #82000). The images shown in Fig. 2 are multichannel overlays of blue (DAPI filter), green (FITC filter) and red (TRITC filter) images. These multichannel images more accurately depict the presence of nematode-associated autofluorescence. Images were recorded electronically using either ORCA or Cool Snap HQ digital cameras (Hamamatsu, Hamamatsu City, Japan and Roper Scientifics, Munich, Germany). Images were recorded on a personal computer using MetaMorph versions 4.5 and 6.2 software (Universal Imaging Corporation, West Chester, PA) and processed for publication using Adobe Photoshop 7.0 and Adobe Illustrator 10.0.

Creating X. nematophila *spheroplasts* in vitro

Xenorhabdus nematophila cells were treated with sucrose/EDTA/lysozyme as described previously (Linstrom *et al*., 1970) to create cell spheroplasts. Briefly, *X. nematophila* cells from 5 ml of stationary-phase (16 h old) LB culture were pelleted by centrifugation and gently resuspended in 10 ml of 20% sucrose-20 mM Tris-HCl (pH 8.0). To this suspension, 0.5 ml of 0.1 M EDTA and 100 µl of 15 mg ml^{-1} lysosyme were added, mixed gently and the suspension allowed to sit on ice for 40 min to digest the bacterial cell wall. Samples were removed directly from this suspension for fluorescence microscopy.

In silico *analysis of* X. nematophila *19061 genome*

To probe the presence of potential metabolic pathways in the *X. nematophila* 19061 genome, protein sequences from *E. coli* and other organisms corresponding to enzymatic steps in known biosynthetic pathways (Green *et al*., 1996; Greene, 1996; Hill and Spenser, 1996; Matthews, 1996; Meganathan, 1996; Patte, 1996; Pittard, 1996; Stauffer, 1996; Umbarger, 1996; Crosa and Walsh, 2002) were compared with the *X. nematophila* genome database using the translated-BLAST (tBLASTn) algorithm (Altschul *et al*., 1997). For each protein sequence probe that was compared with the translated *X. nematophila* 19061 genome, an *E*-value between 0.0 and 1e-90 was considered to represent the presence of a gene with that function in *X. nematophila* (Fig. 2). Known or putative *tonB* genes from other organisms failed to provide an *E*-value within the range given, suggesting that either enterobacterial TonB sequences are divergent or were not present in *X. nematophila*. However, *E. coli* and *Photorhabdus luminescens tonB* genes both showed similarity to a single region of the *X. nematophila* genome (*E*-values of 1e-23 and 1e-38 respectively), allowing us to identify a putative *X. nematophila tonB*. The *X. nematophila* ORF designated as *tonB* in which we constructed a mutation, is syntenic with known or putative *tonB* ORFs from other enterobacteriacea including *E. coli* K12, *Erwinia caratovora*, *Yersinia pestis* and *P. luminescens*, and occurs at an apparently conserved chromosomal locus between the *cls* and *ispZ* ORFs. Additionally, the putative *X. nematophila* TonB contains known features that are characteristic of Gram-negative TonB sequences, a conserved S-X_3-H motif in its N-

terminus as well as a proline-rich interior that contains nine P-E/K motifs (Postle and Kadner, 2003).

Screening for amino acid and vitamin auxotrophs

Libraries of *X. nematophila* mutagenized with Tn*5* and Tn*10* were prepared as described previously using the transposon donor plasmids listed in Table 1 (Heungens *et al*., 2002). Tn-mutants were picked into 96-well plates containing 150 μl of LB + rifampicin per well and shaken at 30°C for 24 h to allow bacterial growth. Samples of individual clones grown in 96-well plates then were transferred to the surfaces of various defined media contained in 86 × 128 mm plates (Nunc, Naperville, IL) using a 96-prong replicator that transfers ~3–5 μl of each bacterial culture. Each set of 96 mutants was replica-plated onto defined medium containing all 20 L-amino acids as a positive control, and then onto other defined media lacking particular amino acids for which auxotrophs were sought. After 48 h of growth, mutants that grew in the presence of all 20 L-amino acids, but failed to grow in the absence of a particular amino acid were considered candidate auxotrophs for the amino acids they required and retested.

To identify the disrupted gene in each auxotroph, genomic DNA was extracted from each mutant using a MasterPure DNA extraction kit (Epicentre, Madison, WI) and individual aliquots digested with ApaI, BamHI, EcoRI, EcoRV, KpnI, PstI, SalI and XbaI. Digested genomic fragments were ligated into pBluescript (Stratagene, La Jolla, CA) cut with the corresponding restriction enzyme, ligations transformed into *E. coli* S17-1 λ *pir* and plated on LB containing antibiotics (kanamycin or chloramphenicol) selective for the particular Tn that was used. Cloned fragments, containing the inserted Tn and flanking genomic regions, were sequenced to identify the point of Tn insertion.

Targeted mutation of metabolic pathways

Targeted mutations of *X. nematophila* genes were constructed in two ways. Mutants with lesions in *serB*, *tonB*, *ubiC*, *menF* and *kbl* were constructed using an insertion-duplication mutagenesis (IDM) approach (Morrison *et al*., 1984). IDMs were constructed using pDel-1KS. Briefly, internal fragments of genes to be disrupted were amplified using primers listed in Table S1, the fragment's ends digested with appropriate restriction enzymes and then cloned into pDel-1KS digested with XbaI and EcoRV. The resulting pDel-1KS-based clones were conjugated from *E. coli* S17-1 λ *pir* into *X. nematophila* HGB081 and single-recombinants selected on LB + kanamycin. Mutants were verified based either on auxotrophic phenotype (*serB*) or using a PCR-based strategy (*tonB*, *ubiC*, *menF* and *kbl*). PCR-based verification was conducted using oligonucleotide pairs that anneal within the *aphA* gene of the inserted pDel1-KS and downstream of the targeted IDM insertion site but outside of the original internal gene fragment amplified. Amplification of this fragment indicates specific insertion of pDel-1KS to the desired chromosomal locus. For single-insertion IDM mutants (*serB*, *tonB*, *ubiC*, *menF* and *kbl*) kanamycin was included in nematode–bacteria coculture on LA medium to maintain selection on mutants during coculture. Additionally, during gross assay evaluation of IJs produced on these mutants, dilutions of IJ sonicates were plated on LB and LB + kanamycin to ensure that colonizing bacteria had retained their respective pDel-1 insertions.

To delete a region of the *X. nematophila* genome containing parts of the neighbouring *tyrA* and *pheA* genes we used a novel two-step IDM approach. First, an internal fragment of *tyrA* amplified using oligonucleotides *tyrA* NC fwd and *tyrA* NC rev, was cloned into pDel-1KS and integrated into the chromosome of HGB081. As anticipated, this IDM mutant was an auxotroph for L-tyrosine. Second, an internal fragment of *pheA* was amplified using oligonucleotides *pheA* NC rev and *pheA* NC fwd, cloned into pKR100B and integrated into the genome of the previously constructed strain containing *tyrA*::pDel-1KS. As anticipated this strain was an auxotroph for both L-tyrosine and L-phenylalanine. This double auxotroph was plated on LB + sucrose and chloramphenicol to select for a recombination event between the adjacent and homologous suicide plasmids, pDel-1KS and pKR100B, resulting in loss of pDel-1KS and deletion of the intervening genomic region containing portions of both *tyrA* and *pheA*. The resulting strain, HGB825, is auxotrophic for L-tyrosine and L-phenylalanine, and contains a pKR100B insertion in place of the deleted *tyrA-pheA* fragment. For construction of HGB826, an identical strategy was employed, except that the *pheA* internal fragment amplified using oligonucleotides *pheA* NC fwd and *pheA* NC rev was cloned into pKR100B-Str instead of pKR100B.

Acknowledgements

We would like to thank Eugenio I. Vivas and Sara A. Gilmore for constructing pSAG1. We also thank Karen Visick (Loyola University of Chicago) for providing pKV124 and Andrew Camilli (Tufts University) for providing pRES1. This work was supported by NIH Grant GM59776, NSF Grant IBN0416783 and USDA/CRES Grant CRHF-0-6055 awarded to H.G.-B. E.C.M. was supported during some of this work by an Ira L. Baldwin Distinguished Predoctoral Fellowship, awarded by the Department of Bacteriology, University of Wisconsin–Madison. F.M.R. was supported through NSF Research Experience for Undergraduates Grant 0138978 (Summer 2003).

References

Alexeyev, M.F., Shokolenko, I.N., and Croughan, T.P. (1995) New mini-Tn*5* derivatives for insertion mutagenesis and genetic engineering in Gram-negative bacteria. *Can J Microbiol* **41:** 1053–1055.

Altschul, S.F., Madden, T.L., Schaffer, A.A., Zhang, J., Zhang, Z., Miller, W., and Lipman, D.J. (1997) Gapped BLAST and PSI-BLAST: a new generation of protein database search programs. *Nucleic Acids Res* **25:** 3389–3402.

Bao, Y., Lies, D.P., Fu, H., and Roberts, G.P. (1991) An improved Tn*7*-based system for the single-copy insertion of cloned genes into chromosomes of Gram-negative bacteria. *Gene* **109:** 167–168.

Bird, A.F., and Akhurst, R.J. (1983) The nature of the intestinal vesicle in nematodes of the family Steinernematidae. *Int J Parasitol* **13:** 599–606.

Couche, G.A., and Gregson, R.P. (1987) Protein inclusions produced by the entomopathogenic bacterium *Xenorhabdus nematophilus* ssp. *nematophilus*. *J Bacteriol* **169:** 5279–5288.

Couche, G.A., Lehrbach, P.R., Forage, R.G., Cooney, G.C., Smith, D.R., and Gregson, R.P. (1987) Occurrence of intracellular inclusions and plasmids in *Xenorhabdus* spp. *J Gen Microbiol* **133:** 967–974.

Cowles, C.E., and Goodrich-Blair, H. (2004) Characterization of a lipoprotein, NilC, required by *Xenorhabdus nematophila* for mutualism with its nematode host. *Mol Microbiol* **54:** 464–477.

Crosa, J.H., and Walsh, C.T. (2002) Genetics and assembly line enzymology of siderophore biosynthesis in bacteria. *Microbiol Mol Biol Rev* **66:** 223–249.

Duncan, K., and Coggins, J.R. (1986) The *serC-aroA* operon of *Escherichia coli*. A mixed function operon encoding enzymes from two different amino acid biosynthetic pathways. *Biochem J* **234:** 49–57.

Earhart, C.F. (1996) Uptake and metabolism of iron and molybdenum. In *Escherichia coli and Salmonella: Cellular and Molecular Biology*, Vol. 1. Neidhardt, F.C. (ed.). Washington, DC: American Society for Microbiology Press, pp. 1075–1090.

Ferraioli, S., Tate, R., Cermola, M., Favre, R., Iaccarino, M., and Patriarca, E.J. (2002) Auxotrophic mutant strains of *Rhizobium etli* reveal new nodule development phenotypes. *Mol Plant Microbe Interact* **15:** 501–510.

Forst, S., and Clarke, D. (2002) Bacteria-nematode symbioses. In *Entomopathogenic Nematology*. Gaugler, R. (ed.). Wallingford, UK: CABI Publishing, pp. 57–77.

Forst, S.A., and Tabatabai, N. (1997) Role of the histidine kinase, EnvZ, in the production of outer membrane proteins in the symbiotic-pathogenic bacterium *Xenorhabdus nematophilus*. *Appl Environ Microbiol* **63:** 962–968.

Graf, J., and Ruby, E.G. (1998) Host-derived amino acids support the proliferation of symbiotic bacteria. *Proc Natl Acad Sci USA* **95:** 1818–1822.

Graf, J., and Ruby, E.G. (2000) Novel effects of a transposon insertion in the *Vibrio fischeri glnD* gene: defects in iron uptake and symbiotic persistence in addition to nitrogen utilization. *Mol Microbiol* **37:** 168–179.

Green, J.M., Nichols, B.P., and Matthews, R.G. (1996) Folate biosynthesis, reduction, and polyglutamylation. In *Escherichia coli and Salmonella: Cellular and Molecular Biology*, Vol. 1. Neidhardt, F.C. (ed.). Washington, DC: American Society for Microbiology Press, pp. 665–673.

Greene, R.C. (1996) Biosynthesis of methionine. In *Escherichia coli and Salmonella: Cellular and Molecular Biology*, Vol. 1. Neidhardt, F.C. (ed.). Washington, DC: American Society for Microbiology Press, pp. 542–560.

Grewal, P.S., Matsuura, M., and Converse, V. (1997) Mechanisms of specificity of association between the nematode *Steinernema scapterisci* and its symbiotic bacterium. *Parasitology* **114:** 483–488.

Hanisch, F.G. (2001) O-glycosylation of the mucin type. *Biol Chem* **382:** 143–149.

Heungens, K., Cowles, C.E., and Goodrich-Blair, H. (2002) Identification of *Xenorhabdus nematophila* genes required for mutualistic colonization of *Steinernema carpocapsae* nematodes. *Mol Microbiol* **45:** 1337–1353.

Hill, R.E., and Spenser, I.D. (1996) Biosynthesis of vitamin B6. In *Escherichia coli and Salmonella: Cellular and Molecular Biology*, Vol. 1. Neidhardt, F.C. (ed.). Washington, DC: American Society for Microbiology Press, pp. 695–703.

Hoiseth, S.K., and Stocker, B.A. (1985) Genes *aroA* and *serC* of *Salmonella typhimurium* constitute an operon. *J Bacteriol* **163:** 355–361.

Hultgren, S.J., Jones, C.H., and Normark, S. (1996) Bacterial adhesins and their assembly. In *Escherichia coli and Salmonella: Cellular and Molecular Biology*, Vol. 2. Neidhardt, F.C. (ed.). Washington, DC: American Society for Microbiology Press, pp. 2730–2756.

Kleckner, N., Bender, J., and Gottesman, G. (1991) Uses of transposons with emphasis on Tn*10*. *Methods Enzymol* **204:** 139–180.

Linstrom, E.B., Boman, H.G., and Steele, B.B. (1970) Resistance of *Escherichia coli* to penicillins. VI. Purification and characterization of the chromosomally mediated penicillinase present in *ampA*-containing strains. *J Bacteriol* **101:** 218–231.

McCann, J., Stabb, E.V., Millikan, D.S., and Ruby, E.G. (2003) Population dynamics of *Vibrio fischeri* during infection of *Euprymna scolopes*. *Appl Environ Microbiol* **69:** 5928–5934.

Martens, E.C., and Goodrich-Blair, H. (2005) The *Steinernema carpocapsae* intestinal vesicle contains a subcellular structure with which *Xenorhabdus nematophila* associates during colonization initiation. *Cellular Microbiology* (in press). doi:10.1111/j.1462-5822.2005.00585.x

Martens, E.C., Heungens, K., and Goodrich-Blair, H. (2003a) Early colonization events in the mutualistic association between *Steinernema carpocapsae* nematodes and *Xenorhabdus nematophila* bacteria. *J Bacteriol* **185:** 3147–3154.

Martens, E.C., Gawronski-Salerno, J., Vokal, D.L., Pellitteri, M.C., Menard, M.L., and Goodrich-Blair, H. (2003b) *Xenorhabdus nematophila* requires an intact *iscRSUA-hscBA-fdx* operon to colonize *Steinernema carpocapsae* nematodes. *J Bacteriol* **185:** 3678–3682.

Martens, E.C., Vivas, E.I., Heungens, K., Cowles, C.E., and Goodrich-Blair, H. (2003c) Investigating mutualism between entomopathogenic bacteria and nematodes. *Nematology Monographs and Perspectives (2): Proceedings of the Fourth International Congress of Nematology* **2:** 447–462.

Matthews, R.G. (1996) One-carbon metabolism. In *Escherichia coli and Salmonella: Cellular and Molecular Biology*, Vol. 1. Neidhardt, F.C. (ed.). Washington, DC: American Society for Microbiology Press, pp. 600–611.

Meganathan, R. (1996) Biosynthesis of the isoprenoid quinones menaquinone (vitamin K2) and ubiquinone (coenzyme Q). In *Escherichia coli and Salmonella: Cellular and Molecular Biology*, Vol. 1. Neidhardt, F.C. (ed.). Washington, DC: American Society for Microbiology Press, pp. 642–656.

Miller, J.H. (1972) *Experiments in Molecular Genetics.* Cold Spring Harbor, NY: Cold Spring Harbor Laboratory Press.

Miller, V.L., and Mekalanos, J.J. (1988) A novel suicide vector and its use in construction of insertion mutations: osmoregulation of outer membrane proteins and virulence determinants in *Vibrio cholerae* requires *toxR*. *J Bacteriol* **170:** 2575–2583.

Mitani, D.K., Kaya, H.K., and Goodrich-Blair, H. (2004) Comparative study of the entomopathogenic nematode, *Steinernema carpocapsae*, reared on mutant and wild-type *Xenorhabdus nematophila*. *Biol Control* **29:** 382–391.

Morrison, D.A., Trombe, M.C., Hayden, M.K., Waszak, G.A., and Chen, J.D. (1984) Isolation of transformation-deficient *Streptococcus pneumoniae* mutants defective in control of competence, using insertion-duplication mutagenesis with the erythromycin resistance determinant of pAM beta 1. *J Bacteriol* **159:** 870–876.

Orchard, S.S., and Goodrich-Blair, H. (2004) Identification and functional characterization of a *Xenorhabdus nematophila* oligopeptide permease. *Appl Environ Microbiol* **70:** 5621–5627.

Parales, R.E., and Harwood, C.S. (1993) Construction and use of a new broad-host-range *lacZ* transcriptional fusion vector, pHRP309, for Gram-negative bacteria. *Gene* **133:** 23–30.

Patte, J.-C. (1996) Biosynthesis of threonine and lysine. In *Escherichia coli and Salmonella: Cellular and Molecular Biology*, Vol. 1. Neidhardt, F.C. (ed.). Washington, DC: American Society for Microbiology Press, pp. 528–541.

Pittard, A.J. (1996) Biosynthesis of the aromatic amino acids. In *Escherichia coli and Salmonella: Cellular and Molecular Biology*, Vol. 1. Neidhardt, F.C. (ed.). Washington, DC: American Society for Microbiology Press, pp. 458–484.

Poinar, G.O. (1966) The presence of *Achromobacter nematophilus* in the infective stage of a *Neoplectana* sp. (Steinernematidae: Nematoda). *Nematologica* **12:** 105–108.

Poinar, G.O.J., and Thomas, G.M. (1966) Significance of *Achromobacter nematophilus* Poinar and Thomas (Achromabacteraceae: Eubacteriales) in the development of the nematode, DD-136 (*Neoplectana* sp. Steinernematidae). *Parasitology* **56:** 385–390.

Popiel, I., Grove, D.L., and Friedman, M.J. (1989) Infective juvenile formation in the insect parasitic nematode *Steinernema feltiae*. *Parasitology* **99:** 77–81.

Postle, K., and Kadner, R.J. (2003) Touch and go: tying TonB to transport. *Mol Microbiol* **49:** 869–882.

Pugsley, A.P., and Reeves, P. (1976) Iron uptake in colicin B-resistant mutants of *Escherichia coli* K-12. *J Bacteriol* **126:** 1052–1062.

Reitzer, L.J. (1996) Sources of nitrogen and their utilization. In *Escherichia coli and Salmonella: Cellular and Molecular Biology*, Vol. 1. Neidhardt, F.C. (ed.). Washington, DC: American Society for Microbiology Press, pp. 380–390.

Schwyn, B., and Neilands, J.B. (1987) Universal chemical assay for the detection and determination of siderophores. *Anal Biochem* **160:** 47–56.

Sicard, M., Ferdy, J.B., Pages, S., Le Brun, N., Godelle, B., Boemare, N., and Moulia, C. (2004a) When mutualists are pathogens: an experimental study of the symbioses between *Steinernema* (entomopathogenic nematodes) and *Xenorhabdus* (bacteria). *J Evol Biol* **17:** 985–993.

Sicard, M., Brugirard-Ricaud, K., Pages, S., Lanois, A., Boemare, N.E., Brehelin, M., and Givaudan, A. (2004b) Stages of infection during the tripartite interaction between *Xenorhabdus nematophila*, its nematode vector, and insect hosts. *Appl Environ Microbiol* **70:** 6473–6480.

Simon, R., Priefer, U., and Pühler, A. (1983) A broad host range mobilization system for *in vivo* genetic engineering: transposon mutagenesis in Gram-negative bacteria. *Biotechnology* **1:** 784–791.

Stauffer, G.V. (1996) Biosynthesis of serine, glycine, and one-carbon units. In *Escherichia coli and Salmonella: Cellular and Molecular Biology*, Vol. 1. Neidhardt, F.C. (ed.). Washington, DC: American Society for Microbiology Press, pp. 506–513.

Taylor, R.T., and Weissbach, H. (1973) N5-Methyltetrahydrofolate-homocysteine methyltransferases. In *The Enzymes*, Vol. IX. Boyer, P.D. (ed.). New York: Academic Press, pp. 121–165.

Thomas, M.G., O'Toole, G.A., and Escalante-Semerena, J.C. (1999) Molecular characterization of *eutF* mutants of *Salmonella typhimurium* LT2 identifies *eutF* lesions as partial-loss-of-function *tonB* alleles. *J Bacteriol* **181:** 368–374.

Umbarger, H.E. (1996) Biosynthesis of the branched-chain amino acids. In *Escherichia coli and Salmonella: Cellular and Molecular Biology*, Vol. 1. Neidhardt, F.C. (ed.). Washington, DC: American Society for Microbiology Press, pp. 442–457.

Visick, K.L., and Skoufos, L.M. (2001) Two-component sensor required for normal symbiotic colonization of *Euprymna scolopes* by *Vibrio fischeri*. *J Bacteriol* **183:** 835–842.

Vivas, E.I., and Goodrich-Blair, H. (2001) *Xenorhabdus nematophilus* as a model for host–bacterium interactions: *rpoS* is necessary for mutualism with nematodes. *J Bacteriol* **183:** 4687–4693.

Whalen, W.A., and Berg, C.M. (1982) Analysis of an *avtA*::Mu *d*1(Ap *lac*) mutant: metabolic role of transaminase C. *J Bacteriol* **150:** 739–746.

Wouts, W.M. (1981) Mass production of the entomogenous nematode, *Heterorhabditis heliothidis* (Nematoda: Heterorhabditidae), on artificial media. *J Nematol* **13:** 467–469.

Xu, J., and Hurlbert, R.E. (1990) Toxicity of irradiated media for *Xenorhabdus* spp. *Appl Environ Microbiol* **56:** 815–818.

Supplementary material

The following supplementary material is available for this article online:

Table S1. Oligonucleotides used in this study.